PR12-17-011

The Parity Violation Parton Distribution Function (PVPDF) Experiment: a new experimental constraint on PDFs
Proposal to JLab PAC 45

Whitney Armstrong[1], Seamus Riordan[1], David Armstrong[2], Todd Averett[2], Wouter Deconinck[2], Fatiha Benmokhtar[3], Pete Markowitz[4], Dustin McNulty[5], Jim Dunne[6], Dipangkar Dutta[6], Latif Kabir[6], Samuel Danagoulian[7], Paul King[8], Julie Roche[8], Abhay Deshpande[9], Krishna Kumar[9], Paul Souder[10], Silviu Covrig[11], Mark Dalton* (contact)[11], Cynthia Keppel (co-spokesperson)[11], David Gaskell[11], David Mack[11], Robert Michaels[11], Eric Pooser[11], Brad Sawatzky[11], Edward Kinney[12], Nobuo Sato[13], Michael Gericke[14], Kent Paschke (co-spokesperson)[15], Darko Androic[16], Mark Pitt[17], and Narbe Kalantarians[18]

[1]Argonne National Laboratory, Argonne, IL 60439, USA
[2]College of William and Mary, Williamsburg, VA 23187, USA
[3]Duquesne University, Pittsburgh, PA 15282, USA
[4]Florida International University, Miami, FL 33199, USA
[5]Idaho State University, Pocatello, ID 83209, USA
[6]Mississippi State University, Mississippi State, MS 39762, USA
[7]North Carolina A&T State, Greensboro, NC 27411, USA
[8]Ohio University, Athens, OH 45701, USA
[9]Stony Brook University, Stony Brook, NY 11794, USA
[10]Syracuse University, Syracuse, NY 13244, USA
[11]Thomas Jefferson National Accelerator Facility, Newport News, VA 23606, USA
[12]University of Colorado, Boulder, CO 80309, USA
[13]University of Connecticut, Storrs, CT 06269, USA
[14]University of Manitoba, Winnipeg, MB R3T 2N2, Canada
[15]University of Virginia, Charlottesville, VA 22901, USA
[16]University of Zagreb, Zagreb, Croatia

[17]Virginia Tech, Blacksburg, VA 24061, USA
[18]Virginia Union University, Richmond, VA 23220, USA

May 22, 2017

Abstract

We propose to measure the parity violating asymmetry in inclusive electron deep inelastic scattering (DIS) from a proton target with 1 GeV^2/c^2 $< Q^2 <$ 3.5 GeV^2/c^2 and $0.1 < x < 0.5$. The measurement will require 38 days of 11 GeV beam at 70 μA on a 20 cm liquid hydrogen target in Hall C. Data will be taken with the spectrometers and detectors constituting the base equipment in Hall C, with the SHMS fixed at 8.5 degrees and 6.5 GeV and the HMS fixed at the minimum angle (10.5 degrees) and 6.4 GeV. This data will provide a new and unique experimental constraint on the parton distribution functions at low Q^2, without any nuclear effects. In particular, this will lead to an improved determination of the strange quark PDF at intermediate x, with implications for understanding of the non-perturbative sea, the proton spin puzzle and for TMDs. There is currently no data that effectively pins down the strange quark PDF in the x range of this proposed measurement, leading to extractions that vary over an order of magnitude between various fits.

*dalton@jlab.org

Contents

1 Executive Summary

Quantitatively describing the structure of nucleons in terms of the fundamental, underlying partonic constituents encoded in Quantum Chromodynamics (QCD), our theory of the strong force, remains a defining challenge for hadronic physics research. An ultimate goal is to describe the complete spatial, momentum, spin, flavor, and gluon structure of the nucleon. Parton distribution functions (PDFs) form the basis for the description of the flavor structure of the nucleon. They are central to many of the phenomenological applications of QCD. Because the PDFs are universal, the same PDFs appear in all reactions. They can be measured in a limited set of reactions and then perturbative calculations of hard scattering and PDF evolution enable us to predict, from first principles, cross sections for many other processes. The success of this approach is well known. However, this success is constrained by our ability to measure the PDFs. In the global analysis of PDFs, the partonic degrees of freedom must be matched to the constraining power of the available input experimental data within the adopted theoretical framework, in order for the results to be meaningful. Although global analyses of PDFs have been in progress for over three decades, certain components of the partonic structure of the nucleon are still poorly determined. Foremost among these is the strangeness sector where there are little to no available measurements to constrain the PDF.

The strange-quark parton distribution function (PDF) is a fundamental property of the nucleon and knowing it, to reasonable precision, is an important part of understanding nucleon structure. The measurement described in this proposal will allow rather direct access to this PDF for the first time When included in global fits it will allow the strange quark PDF to be extracted with greatly improved accuracy. Beyond its importance as a fundamental quantity, the strange quark PDF enters into various important residual questions in nuclear physics.

- What is the origin of the *non-perturbative sea*? The non-zero $\bar{d}-\bar{u}$, which cannot be generated perturbatively from gluon radiation has two competing explanations, chiral symmetry breaking, and hadronic fluctuations (pion, kaon cloud effects). Knowledge of the strange distributions is a vital component of understanding the effect.
- What is the resolution of the *spin puzzle*? The low value of the proton spin contributed by quarks may be due to a large negative contribution made by strange quarks. The polarized strange distribution, which is largely still unknown can be further constrained by the strange distribution through the positivity bound.
- Theoretical descriptions of *transverse momentum distributions*, central to the JLab 12 program require precise input of the sea distribution.

The kinematics are chosen to achieve the lowest values of x possible with $Q^2 > 1$ GeV^2/c^2. The strange PDF is interesting in this range of x as it is expected to rise sharply, it shows a very large discrepancy in the extraction by various groups, and will receive the least coverage by future data sets. The strange quark is also the most accessible in this region because this is where the down quark distribution is most well known.

This important data can be obtained with a relatively short measurement using standard equipment in Hall C. The experimental requirements are for a parity violation

experiment. Some data acquisition development will be required. A detailed study of the systematics projects an uncertainty of 1.1 %, dominated by knowledge of the spectrometer angle and by beam polarimetry. This is well matched to the statistics of the measurement in the low x region, where we are most sensitive to strange quarks.

This experiment is complementary to existing data from the LHC which is directly sensitive to strange quarks, but only at lower x. It is also complementary to future data from the SoLID experiment since that data will be at different kinematics, particularly higher x, where the valence quarks are more dominant. The bulk of the data in this experiment will be taken at values of x not expected to be reached by other experiments. It will, therefore, provide critical input to global fitting efforts which require a range of (x, Q^2) data to constrain the PDFs.

2 Physics Motivation

Enormous progress has been made over the last two decades in describing high-energy reactions involving lepton-hadron, hadron-hadron and lepton-lepton collisions in the context of perturbative QCD (pQCD) [1]. The theoretical foundations are based on QCD factorization theorems, which state that experimental cross sections can be described in terms of pertubatively calculable hard coefficients and process-independent, nonperturbative parton distribution functions (PDFs) [2]. At present, such functions are not calculable from first principles but are instead extracted from experimental data using a procedure known as *global QCD analysis*. Although recent advances in lattice QCD have enabled the first ab initio calculations of PDFs to be performed, these are still at a rather early stage and not yet at the point of being useful for phenomenological applications [3].

PDFs, denoted as $f(x, Q^2)$, can be interpreted as probability densities of the longitudinal momentum fraction x of quarks and gluons relative to their parent hadron momentum. They also depend on the scale that characterizes the typical large scale in the reaction (the invariant mass of the virtual photon exchange in DIS, Q^2). The scale dependence is a consequence of factorization and accounts for the inclusion of multiple-gluon radiation that can be absorbed in the PDFs order by order in perturbative QCD. Such effects are encoded in what is known as the DGLAP evolution equations.

Currently a number of groups around the world are engaged in performing global analyses in order to precisely determine the partonic distributions from a large number of observables from many different experiments. This has been partly motivated by the fact that PDFs are universal ingredients in describing particle reactions in facilities such as the Larger Hadron Collider (LHC), where searches beyond the Standard Model via precision electroweak measurements (for example, in the determination of the Higgs couplings) are typically limited by the uncertainties on the PDFs. These global analyses differ in which input data they choose to use, the parameterization of the PDFs, the treatment of heavy quarks, the value of α_s, the way that experimental errors are treated, and the way that theoretical errors are estimated.

Since the early observations by the European Muon Collaboration (EMC) at CERN that hinted at a $\bar{d} - \bar{u}$ asymmetry [4, 5], which was later confirmed by the FNAL E886 experiment [6], the study of PDFs at large-x has played a significant role in nucleon structure to clarify the origin of such asymmetries. Since the latter cannot be explained within perturbative QCD, the phenomenon is intrinsically of non-perturbative origin.

Several models and interpretations exist in the literature that associate the effects with chiral symmetry breaking or hadronic fluctuations [7, 8, 9]. Therefore precise determination of the nucleon sea at large x is vital for understanding the microscopic nature of quarks and gluons inside the proton.

The role of strange quarks in generating the structure of the nucleon provides a key testing ground for our understanding of Quantum Chromodynamics (QCD). Because the nucleon has zero net strangeness, strange observables give tremendous insight into the nature of the vacuum; they can only arise through quantum fluctuations in which strange-antistrange quark pairs are generated. The parton distribution functions (PDFs) of the strange quarks are of special interest as they describe important features of the structure of the nucleon sea, and constrain models of its origin. In addition, their distributions are also important, for instance, because of their impact on quantitative calculations of certain key short-distance processes at hadron colliders.

The transverse momentum distribution (TMD) of quarks and gluons inside hadrons can be accessed by measuring distributions of final state hadrons in semi-inclusive DIS (SIDIS). This is a main focus in the upcoming JLab 12 program. Formally, the transverse momentum of the observed hadron receives contributions from intrinsic transverse momentum of the quarks and gluons as well as from gluon radiation that recoils against the observed hadron. As a result, TMD observables are described theoretically within the so called $W + Y$ construction [1]. The W term is associated with small transverse momentum while the Y term is associated with large transverse momentum. The collinear parton densities enter in both terms. A theoretical expectation from Chiral symmetry breaking is that the sea TMDs have a characteristic width that is larger than the valence distribution. Thus, precise determination of TMDs requires a solid knowledge of sea PDFs, specially in the large x region in order to understand the origin of non-perturbative sea.

Another aspect of nucleon structure is characterized by spin-dependent parton distribution (SPDFs), denoted as $\Delta f(x, Q^2)$, which provide insight to the spin decomposition of the proton. Early observations from the EMC experiment found a relatively small quark contribution to the total spin of the proton [10]. Today experimental facilities like JLab, RHIC-spin and COMPASS at CERN are dedicated to measuring polarization observables in order to better determine the SPDFs. In terms of the "helicity" basis, PDFs and SPDFs can be expressed as

$$f(x, Q^2) = f^{\uparrow}(x, Q^2) + f^{\downarrow}(x, Q^2) \tag{1}$$

$$\Delta f(x, Q^2) = f^{\uparrow}(x, Q^2) - f^{\downarrow}(x, Q^2) \tag{2}$$

where $f^{\uparrow}(x, Q^2)$, $f^{\downarrow}(x, Q^2)$ are interpreted as the momentum distribution of quarks and gluons with positive and negative helicities respectively. Since the helicity distributions are strictly positive definite, one finds the so-called *positivity constraint*:

$$|\Delta f(x, Q^2)| < f(x, Q^2).$$

Like the unpolarized strange distribution, its polarized counterpart is not well known and at present is only accessible through the semi-inclusive measurements of Kaon production in electron-proton scattering. However, these measurements have such large uncertainties that the polarized strange distribution remains elusive. Through the positivity constraint, measurements of the unpolarized strange distribution can provide valuable constraints to the polarized strange distribution.

Much remains to be understood about PDFs in certain regions of x, in particular the strange distribution at intermediate to large x since there are no measurements with direct sensitivity in such region. Although inclusive neutrino DIS, $\nu A \to \mu + X$ [11, 12], can provide some constraints, final state interactions are not well understood, and thus the extraction of the strange distribution is unreliable. Recently, measurements of $W + c$ at the LHC [13, 14] have become available, which directly constrain the strange distribution. However these measurements provide sensitivity to the strange distribution only in the low-x region, typically $x < 0.1$, while leaving the intermediate to large-x strange PDF without direct constraint.

There is therefore the need for an observable with sensitivity to the strange distribution, that accesses the relatively unconstrained region at intermediate to high x. Parity violation in electron scattering is able to provide just such an observable.

2.1 PVDIS Data and the Strange PDF

In the Bjorken limit the parity violating asymmetry, $A_{\rm PV}$ can be expressed as [15]

$$A_{PV} = \frac{G_F Q^2}{4\sqrt{2}\pi\alpha_{\rm em}} \left[a_2(x) + \frac{1-(1-y)^2}{1+(1-y)^2} a_3(x) \right], \tag{3}$$

where $y = \nu/E$, and $a_2(x)$ involves the vector-quark and axial-electron currents, while $a_3(x)$ involves the axial-quark and vector-electron currents, in the interference term

$$a_2(x) = -2\, g_A^e\, \frac{F_2^{\gamma Z}(x)}{F_2^{\gamma}(x)} = \frac{2 \sum_q e_q\, g_V^q\, q^+(x)}{\sum_q e_q^2\, q^+(x)}, \tag{4}$$

with $g_V^u = \frac{1}{2} - \frac{4}{3}\sin^2\theta_W$, $g_V^d = -\frac{1}{2} + \frac{2}{3}\sin^2\theta_W$ [16], $g_A^e = -\frac{1}{2}$, and $q^+(x) = q(x) + \bar{q}(x)$, and

$$a_3(x) = -2\, g_V^e\, \frac{F_3^{\gamma Z}(x)}{F_2^{\gamma}(x)} = -4\, g_V^e\, \frac{\sum_q e_q\, g_A^q\, q^-(x)}{\sum_q e_q^2\, q^+(x)}, \tag{5}$$

with $g_V^e = -\frac{1}{2} + 2\sin^2\theta_W$, $g_A^u = -g_A^d = \frac{1}{2}$ [16] and $q^-(x) = q(x) - \bar{q}(x)$. The strange quarks have down charges $e_s = e_d$, $g_V^s = g_V^d$, and $g_A^s = g_A^d$. The parton model expressions for the structure functions [16] have been used

$$F^{\gamma Z} = 2\,x \sum\nolimits_q e_q\, g_V^q\, q^+, \quad F^{\gamma} = x \sum\nolimits_q e_q^2\, q^+. \tag{6}$$

The parity violating structure function, $F^{\gamma Z}$, has a different flavor structure from that of F^{γ}. In ordinary DIS the d and s contributions are suppressed relative to the u since $e_d^2 = 1/9$ while $e_u^2 = 4/9$. On the other hand, in the parity violating asymmetry these contributions are weighted approximately equally, $e_d\, g_V^d \approx e_u\, g_V^u \approx 1/9$ using $\sin^2\theta_W \approx 1/4$.

In Figure 1, the strange distribution from several PDF fitting global analyses is presented. Throughout this proposal, PDFs from published fits are obtained through the LHAPDF package [17], which is a general purpose C++ interpolator, used for evaluating PDFs from discretized data files. As is clear, the distributions vary by more than an order of magnitude in the region of $x \sim 0.1$, illustrating the current difficulty in determining the strange PDF. The spread from the various analyses can be

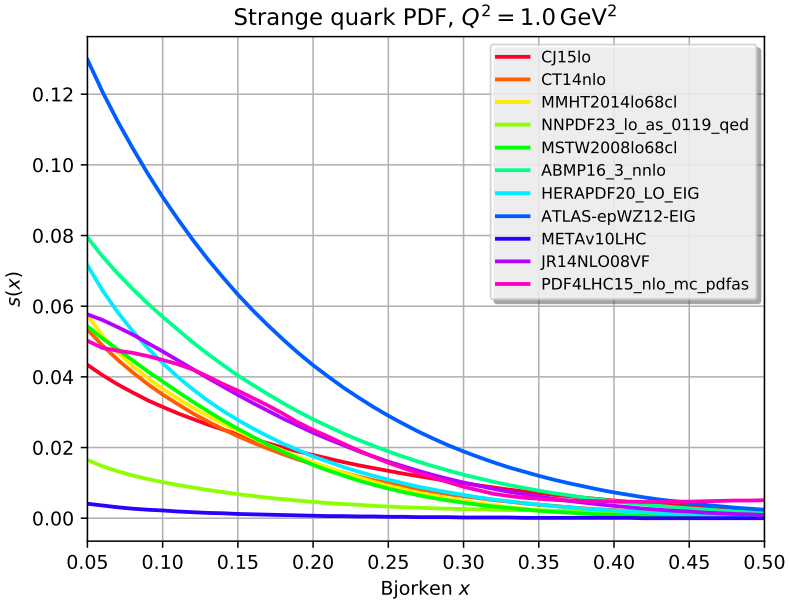

Figure 1: Strange quark PDF from various fits showing a large scatter. For clarity, only the central values are displayed.

viewed as the current theoretical and systematic uncertainty in the extractions, which is significantly larger than the reported uncertainty for most of the fits. Figure 2 shows the strange PDF with these reported uncertainty bands. For clarity, the figure is limited to 4 of the PDF fits which were chosen to represent both the largest and smallest reported uncertainties. Given the scatter in the central values, only the NNPDF and PDF4LHC fits can be said to have uncertainties that encompass the spread of acceptable models. Without data to constrain the fits, the s quark extraction must be obtained largely from the momentum sum rule fitting constraint and is therefore subject to substantial uncertainty, essentially unknown. This indicates the need for an observable, such as PVDIS, that is directly sensitive to the strange distribution in the region of $x \sim 1$

The kinematics of the proposed experiment are $1 \leq Q^2 \leq 3.5$ and $0.1 \leq x \leq 0.5$. This region is subject to finite Q^2 corrections stemming from higher twist effects and target mass corrections [18, 19, 20, 21], which need to be taken into account in order to reliably extract the PDFs. The task of reliably constraining $s(x)$ (and $\bar{s}(x)$) must be performed within the context of a comprehensive global QCD analysis. This is because, beyond leading order in perturbative theory, QCD dynamics strongly couples the strange degrees of freedom to the gluon and the other quark flavors. No parton flavor can be determined in isolation; all available high precision data that constrain the light degrees of freedom are needed in the analysis.

In particular, the CJ (CTEQ-Jefferson Lab) Collaboration[1] includes such corrections in their analysis [22], and allows for the inclusion of low Q^2 data. Within this framework the proposed measurement will play a significant role in pinning down the strange distribution.

[1] https://www.jlab.org/theory/cj/

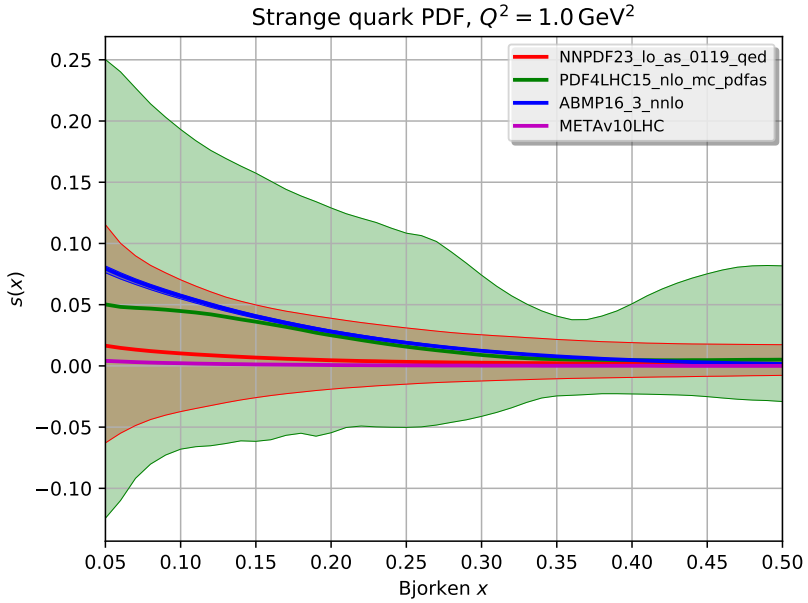

Figure 2: Strange quark PDF from 4 fits plotted with 1σ uncertainties. The fits were chosen to represent both the large and small reported uncertainties. The smallest uncertainties are not visible by eye.

2.2 Projected Results

Using the same set of PDFs as Figure 1, the parity violating asymmetry A_{PV} is calculated for each set using Equation (3) [23] for $q \in \{u, d, s\}$. These predictions, made at $Q^2 = 1$ GeV^2/c^2, can be seen in Figures 3 and 4 along with the points depicting the uncertainties for the proposed measurement. The data projections were obtained from simulation, using the cross section for DIS scattering from a fit to data [24] and the acceptance determined using the "single-arm" Monte-Carlo routines from SIMC[2]. For the purposes of these plots, the simulated data from the two spectrometers was combined and filled in bins of equal size in Bjorken x, plotted at $\langle x \rangle$ for each bin. The final data will be binned differently, as described in Section 3.2, but contain the same statistical power.

Figure 3 shows only the central value of the asymmetry predictions. The asymmetry has been scaled by the factor

$$\eta_{\gamma Z} = \left(\frac{G_F M_Z^2}{2\sqrt{2}\pi\alpha}\right)\left(\frac{Q^2}{Q^2 + M_Z^2}\right)$$

to remove the leading kinematic dependence. It can be seen that there is 7 % difference in the overall scale of the asymmetry between different PDF sets. In addition there are significant differences in the shapes of the asymmetry with x, which is caused by differences in the shapes of the underlying PDF distributions. As described Section 3, the systematic uncertainty 1.1 % systematic, which will provide a significant constraint

[2] https://hallcweb.jlab.org/wiki/index.php/Monte_Carlo

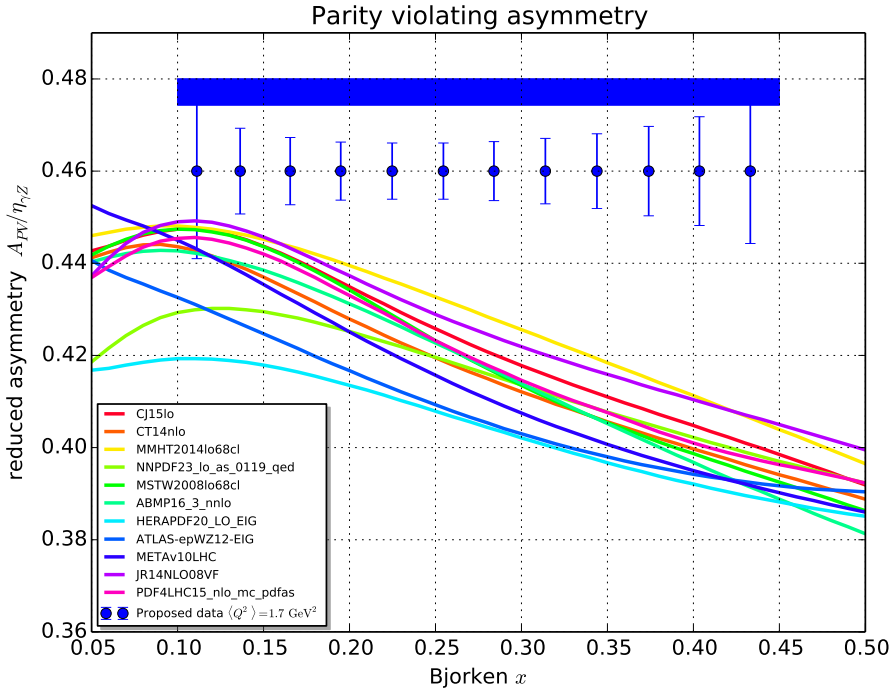

Figure 3: Reduced asymmetry versus Bjorken x for various PDF sets, calculated at leading order using Equation (3) with $q \in \{u, d, s\}$ and PDFs obtained from LHAPDF [17] at Q^2 =1 GeV^2/c^2. The data proposed in this experiment are plotted with statistical uncertainties only, at a constant asymmetry value, and have $\langle Q^2 \rangle = 1.7$ GeV^2/c^2. The expected total systematics uncertainty, assumed to common, is plotted as a blue band at the top.

on the underlying PDFs that are responsible for the disparate predictions for the asymmetry, particularly the strange.

Figure 4 is the same as Figure 3 but includes also the uncertainty with correlations between flavors included using the Hessian eigenvectors or Monte Carlo replica information from LHAPDF. The figure is limited to 5 fits for clarity. It can be seen that different fits have uncertainties with vastly different sizes, with some significantly smaller than the scatter between the fits.

The strange quark PDF is not directly constrained by data, with the exception of neutrino data which has significant interpretation uncertainties. This can dealt with by fixing the strange quark PDF or fitting it with very few degrees of freedom and relying on the momentum sum rule as the primary constraint. For example, in the CJ15 fit, the strange quark distribution is set as $s = \bar{s} = 0.4\,(\bar{u} + \bar{d})$. Since the up and down sea quarks are relatively well determined in the fits, such a formulation reports a small uncertainty on s which does not attempt to express the uncertainty in this underlying assumption. The very small uncertainties in certain fits in Figure 4 therefore indicate the presence of assumptions or ansatz which limited the freedom of the global fit, rather than constraints due to data. The scatter between the central values of the fits is thus a lower bound on the uncertainty in the observable. The data

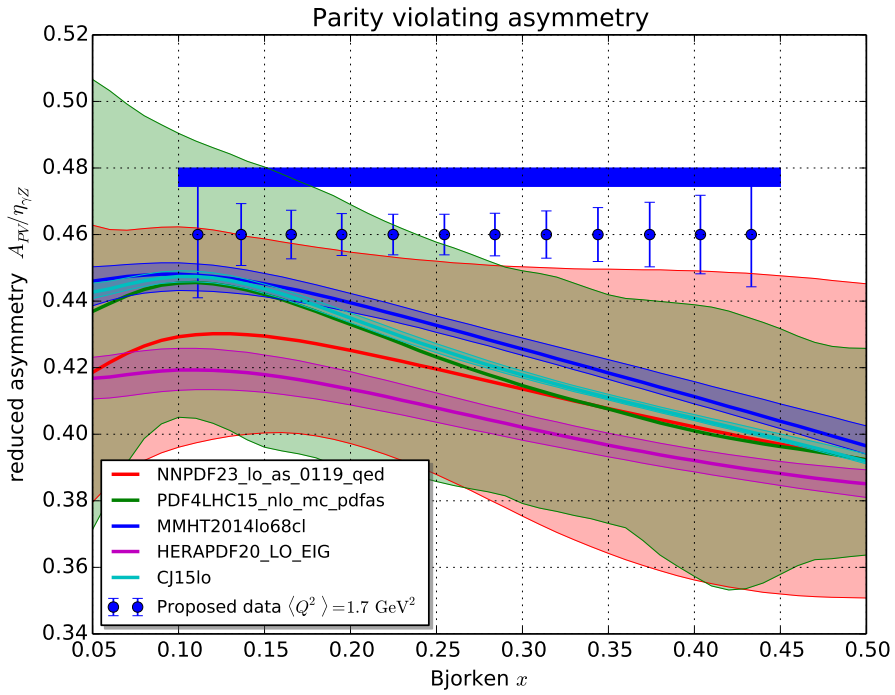

Figure 4: Same as Fig. 3 with errors on the observable calculated using the Hessian eigenvectors or Monte Carlo replica information from LHAPDF. For clarity, only 5 fits are shown.

proposed in this experiment will allow the fits to be performed with more freedom given to the strange quark PDF. This will allow information on the shape of the distribution to be extracted along with information on the magnitude.

The true power and importance of this experiment is seen in the uncertainties of the PDF4LHC fit which tries to provide a realistic PDF model/theoretical uncertainty from a range of considered PDF global fitting efforts. On the scale of those uncertainties, the data proposed in this experiment will have a major impact in constraining the most uncertain of the underlying distributions, namely the strange.

3 Proposed Measurement

3.1 Introduction

The measurement will require beam of 70 uA at the maximum available energy with maximum longitudinal polarization—transverse polarization minimized. We have assumed a polarization of 85 %. This will be incident on a 20 cm, GMP-style, liquid-hydrogen target with a large 4x4 mm raster. A helicity flip rate of up to 240 Hz with delayed reporting will be required. The usual charge feedback from beam current measured in the hall will be implemented. Regular changes of the state of the Insertable Half-Wave Plate (IHWP), expected once per shift, will be required to cancel helicity correlated differences. The helicity magnets in the injector will be used to further

diminish the position and angle differences. Both of the existing polarimeters in Hall C will be used to obtain polarimetry at level of the Qweak experiment. Both the Super High Momentum Spectrometer (SHMS) and the High Momentum Spectrometer (HMS) will be used at small angles, 8.5 degrees and 10.5 degrees respectively. Commissioning data will be taken with full tracking to precisely determine the kinematics of the scattering. The asymmetry measurement itself will include only the lead glass calorimeters and Heavy Gas Cherenkov detectors.

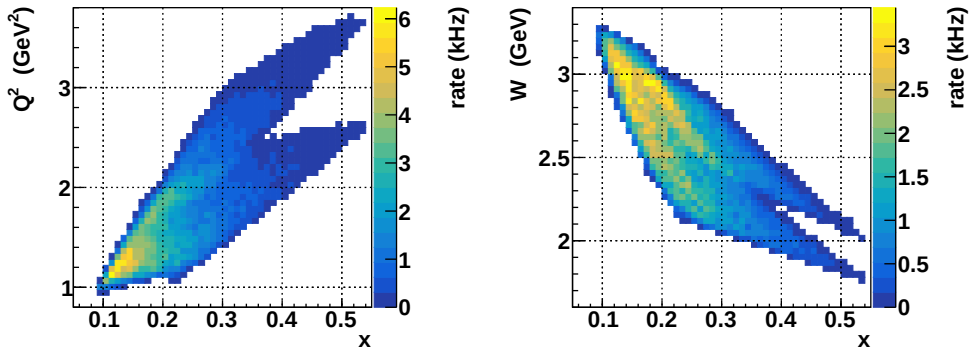

Figure 5: Combined rate of DIS events in the two spectrometers, shown as a function of kinematic variables x, Q^2 and W.

Figure 5 shows the rate of DIS events in the two spectrometers combined. Table 1 gives the spectrometer central setting, averages for each spectrometer and the expected average asymmetry. The kinematics were chosen to reach the lowest values of x achievable while still remaining in the DIS region defined as $Q^2 > 1$ GeV^2/c^2 and $W^2 > 4$ GeV^2/c^2. These kinematic limits were obtained in consultation with the CJ Collaboration and correspond to the kinematic limits they plan to apply to future PDF fits.

Spectrometer	P_{cent} (GeV/c)	θ_{cent} (deg)	$\langle Q^2 \rangle$ (GeV^2/c^2)	$\langle x \rangle$	$\langle W \rangle$ (GeV)	$\langle A_{\text{PV}} \rangle$ (ppm)
HMS	6.4	10.5	2.31	0.275	2.66	185
SHMS	6.5	8.5	1.53	0.209	2.64	122

Table 1: Spectrometer nominal settings, average kinematics in acceptance and estimate of the average asymmetry.

Given the choice of kinematics, Table 2 shows the predicted rate of various components of the flux in each spectrometer. The acceptance was obtained from simulation using the single arm Monte-Carlo routines from SIMC. Accepted events were weighted with appropriate cross sections to determine the rate in the spectrometer. For DIS this is from a fit to data [24], for the elastic tail this is radiated following the prescription of Mo and Tsai [25], for the pion and pair production backgrounds this is from the Wiser fit [26]. More details can be found in Section 3.8.

Spectrometer Rate (kHz)	DIS	elastic tail	π^-	charge symm.	Al windows	total
HMS	173.9	2.8	73.0	1.0	7.3	258.1
SHMS	608.1	17.6	344.0	5.0	26.1	1000.8

Table 2: Rate in kHz of each of the components of the total flux in the spectrometer. Details in Section 3.8.

At worst we expect a π/e ratio of 0.6, therefore only modest pion rejection is required. Currently we intend to use C_4F_{10} as the medium for the SHMS Heavy Gas Cherenkov and the HMS Cherenkov. We will investigate the use of CO_2 which might work better for e/π separation in the SHMS at these energies [27]. We do not plan on using the SHMS Nobel Gas Cherenkov.

3.2 Binning Strategy

During the asymmetry measurement, the tracking detectors will be turned off and only the calorimeters and the Cherenkov detectors will be used for data taking. Each particle incident in the spectrometer that passes through the detectors will have its position in the calorimeter and a measure of its PID determined online. These values will not be read out on an event-by-event basis but will be integrated in what can be thought of as a 4-dimensional histogram, with 2 axes of position and 2 axes of PID.

The position within the SHMS calorimeter is directly available from which blocks receive signal, since it has a fly's eye geometry. The position within the HMS is obtained in the dispersive direction by which block is hit and in the orthogonal direction can be determined from timing difference between the two PMTs on the end of each block in the first 2 layers or from the vertical scintillator that fires. Figures 6 and 7 show how the kinematics vary across the calorimeter at a 10 cm resolution. Each bin in position across the calorimeter will have values of x and Q^2 determined from tracking. One PID value will be the signal size in the Cherenkov detector and the other will be determined from the relative size of the pre-shower and shower detectors in the calorimeter.

3.3 Data Acquisition and Dead-time

When considering the high rate requirements of this proposal there are 2 main issues, pileup or occupancy within the detectors and dead-time in the DAQ system. We anticipate very little dead-time from the DAQ itself due to it being a "pipeline" system.

Both the lead glass calorimeter and the gas Cherenkov detectors are relatively fast, recovering within 50 ns after an incident particle. Assuming 50 ns occupancy dead-time and 1 MHz rate gives a naive dead-time due to pileup in the detectors of $\sim$5 %. In practice, there is a high degree of segmentation within the detector stack and the rate is spread over many detectors, so that the effective occupancy will be lower. The SHMS Cherenkov will experience the highest rate per channel. There are 4 mirrors, each with a dedicated PMT, but many particles deposit light in more than one PMT so it is difficult to estimate the true occupancy. This can be determined most easily from data taken during early 12 GeV experiments.

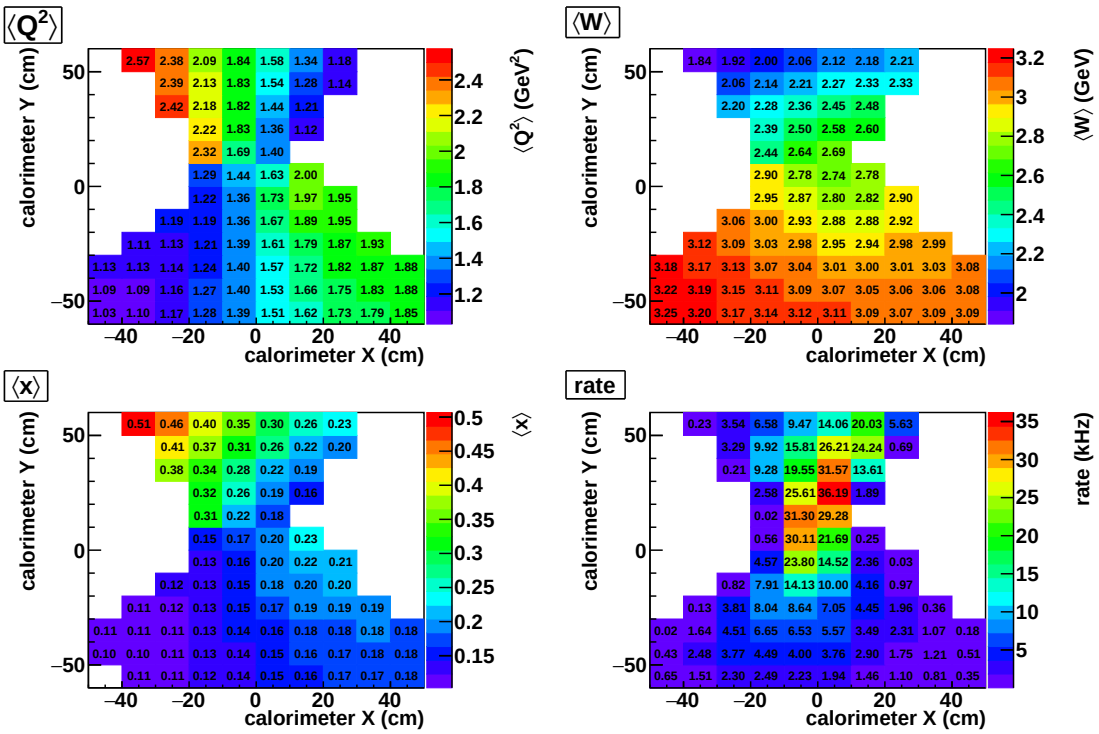

Figure 6: Kinematics of DIS events incident on the lead glass calorimeter in the SHMS as a function of the position on the calorimeter face. For illustration the bins are 10 cm wide (10 × 12).

The existing readout system in Hall C is fully-pipeline capable, composed of F250 FADCs, CAEN 1190 TDCs, and a full complement of JLab modern Trigger Interface (TI), Trigger Supervisor (TS), Signal Distribution (SD), and Crate Trigger Processor (CTP) supporting hardware. These may in principle be used at high rate without any intrinsic dead-time of their own. Using an FPGA based system allows logic combinations which can be much more sophisticated than practical with NIM. This experiment will require the CTP to be replaced with the more capable VXS Trigger Processor (VTP).

The VTP contains more backplane serial links to front-end payload modules, more fiber optics serial links to other crates, and more FPGA resources for trigger logic. The VTP has ∼4 MB of fast memory and is planned to have ∼1 GB/s readout capability developed within the next few years. The F250 modules will continuously feed their data to the VTP along the VXS backplane. The VTP would run algorithms to detect pulses, determine the geometrical center in the calorimeter and determine the PID parameters from the Cherenkov and calorimeter detectors. Two data histograms would be stored on the VTP, one being filled during a window while the other one is read out. We budget ∼1 MB of the fast memory per histogram leaving the remainder for algorithmic use. This would allow a histogram with 16 bit depth (counts up to 65536) to be 26 bins in each of the 4 dimensions—more than adequate for the resolution and range of the position and PID quantities. The expected 240 MB/s rate fits easily within readout capability of the VTP.

Custom firmware will be required to implement the scheme as described. The JLab

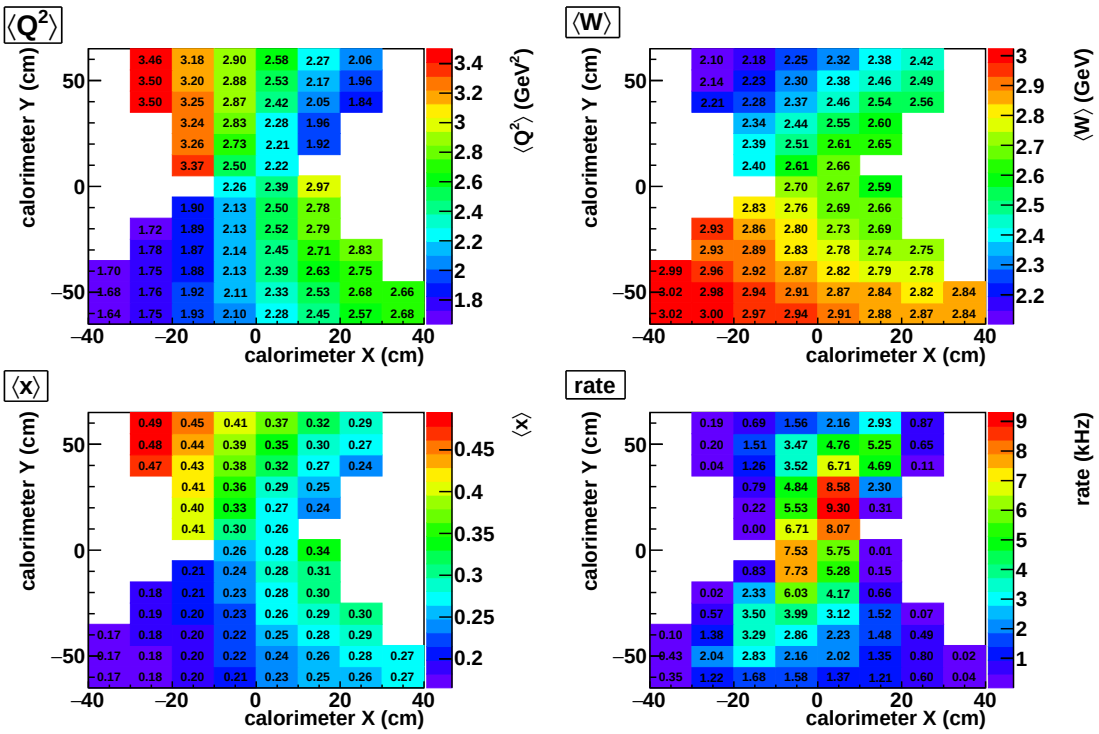

Figure 7: Kinematics of DIS events incident on the lead glass calorimeter in the HMS as a function of the position on the calorimeter face. For illustration the bins are 10 cm wide (8×13).

Fast Electronics group maintains the expertise for developing firmware at JLab and they would be asked to develop the firmware for this experiment too. They have already produced custom firmware for the HPS, CLAS and GlueX Experiments which has worked successfully.

Since any dead-time affects the measured asymmetry, the imperative is to minimize, accurately measure and monitor the dead-time due to pileup in the detectors. The dead-time will be continuously measured and monitored by injecting pulses into the data and monitoring for them to arrive in the analysis. This will be done during the $\sim$50 μs of time available between integration windows when the beam polarization is being changed, so as not to interfere with the asymmetry measurement. Assuming one pulse per transition gives $\sim$20 million per day, allowing high statistics real-time monitoring of the overall dead-time measurement and high statistics measurement of the dead-time in each bin over the whole experiment.

Another powerful way to measure and monitor the pileup is to take dedicated data runs where the full waveforms for each hit are read out, exploiting a natural capability of the F250. Analyzing these waveforms offline will allow a very sophisticated analysis of any pileup in the detector. Hall D was able to take full waveform data at an event rate of $\sim$3 kHz and data rate $\sim$800 MB/s. With a significantly smaller payload we expect to easily exceed this event rate. Additional dedicated data taking, such as beam current scans, threshold scans and charge asymmetry scans will be used to study nonlinearities in the dead-time and other general rate-dependent effects.

Using these two techniques will easily allow measuring the dead-time to a level of

5 %, giving a very conservative uncertainty of 0.25 %. We budget 30 minutes per day to take full-waveform pileup measurements, a total of 16 hours, and an additional 4 hours for dedicated beam current and charge asymmetry scans.

3.4 Tracking and Q^2 Determination

In the 6 GeV era, the spectrometer angle and momentum were constrained by a large body of H$(e, e'p)$ data, leading to high precision [28]. Such studies are planned for the upcoming experiments to be run in 2017/2018 in Hall C. We expect to be able measure the beam energy to 0.1 % and expect an uncertainty on the absolute scattered momentum of 0.1% and the scattered angle of 0.5 mrad. These uncertainties lead to an overall uncertainty on Q^2 of 0.72 % dominated by knowledge of the scattering angle.

We intend to take data on a point target, a multi-foil target and sieve slit data in order to verify the spectrometer calibrations. Elastic scattering data will also be taken with a water target, at lower beam energy, in order to minimize uncertainty in the spectrometer angle. The water target will require removal before the use of the cryogenic target, and a beam pass change. High statistics counting mode data will be taken in dedicated low current running with the production target and full tracking chambers. This will be repeated a few times through the experiment. We budget 6 shifts for taking tracking mode data.

3.5 Polarimetry

A high level of precision is required in measurement of the beam polarization in order to match statistical precision. We aim for a combined uncertainty on the polarization for our two polarimeters of 0.6 %, as explained in this section. In order to achieve this level of polarimetry, this experiment will use the same strategy successfully employed during the Qweak experiment. The polarization will be measured by both the existing Compton and Møller polarimeters in Hall C.

During the Qweak experiment, the Compton polarimeter in Hall C measured the polarization with uncertainty of 0.59 % [29] at a beam energy of 1.16 GeV. At the 11 GeV beam energy of this proposal, the asymmetry is significantly larger, making the measurement easier. The asymmetry has a distinct shape as a function of energy exchanged from electron to photon, described by QED. It is a maximum at maximum energy transfer (endpoint), decreases with energy, changes sign and rises with opposite sign to the lowest values of energy transfer. The Compton chicane has been made shallower meaning that the existing electron detector, which is 20 mm long, will still capture about half of the scattered spectrum—almost to the asymmetry zero crossing. This will allow the same asymmetry spectrum shape-fitting analysis procedure to be used.

In addition, the dominant source of systematic uncertainty from the previous measurement can be improved upon by developing new firmware for the CAEN V1495 boards that process the data [29]. We budget a setup and commissioning time, which will include beam tuning through the chicane, of 2 shifts. Recommissioning of the Compton will be helped by the ability to send beam through the chicane prior to the experiment, for example parasitically during a preceding beam time, in order to verify all systems.

	E_{beam}	endpoint asymmetry	Distance from beam endpoint	asymmetry zero
Qweak	1.16 GeV	0.04	17 mm	9 mm
PVPDF	11 GeV	0.32	36 mm	18 mm

Table 3: Comparison of Compton polarimetry parameters for the Qweak experiment and this proposal.

Detailed simulations indicate that the Møller polarimeter will be able to achieve an uncertainty of 0.74 % at 11 GeV.[3] Achieving this level of uncertainty will require dedicated measurements interspersed throughout the experiment. We anticipate Møller measurements every 3 days, each of will take about 4 hours, which gives a total of 40 hours or 5 shifts.

The collaboration is familiar with the challenges of high precision polarimetry and is committing to getting the polarimeters operating at the necessary level. We assume a combined uncertainty, for the 2 polarimeters, of 0.6 % on the polarization.

3.6 Helicity Correlated Differences

The sensitivity to the typical helicity correlated beam differences observed at CEBAF will be small since the physical asymmetries of interest are large, ∼130 ppm. In addition the effect will be smaller than elastic scattering experiments since the rates and asymmetries from inelastic scattering are more slowly varying with energy and angle than elastic scattering.

We will use feedback on charge in the source based on measurements with the hall BCM in order to drive the cumulative charge difference to zero. Beam differences off the photocathode will be minimized through a careful setup of the polarized source [30]. The helicity magnets in the injector will be used to further diminish the position and angle differences. Regular changes of the state of the IHWP will be used to help cancel the remaining differences. We will perform regular modulation of the beam position and energy as was done in the Qweak experiment [31], using the existing hardware in the Hall C beamline, in order to extract the true sensitivity of the detectors to beam energy, position and angle changes. This response will allow measured beam differences to be corrected. The experiment will not request a Wien reversal to mitigate beam spot size asymmetries, since the expected size of these effects, as bounded by studies done at the electron source, are too small to be of concern here.

Table 4 lists the sensitivity of the scattering rate to changes in beam position, angle and energy, as determined from simulation. Using the techniques described above we intend to hold the beam position difference to < 20 nm, angle difference to < 4 nrad and energy difference to < 100 ppb on average over the experiment. These differences are not as small as what was achieved in either the suite of HAPPEX experiments or Qweak, and are expected to be readily achievable. This represents a total correction of < 0.6 ppm which is ~ 0.5 % on our expected asymmetry. Assuming an uncertainty in these corrections of around 20 %, the total uncertainty contribution to the experiment due to beam differences is ~ 0.1 %.

[3] Kamilah Walker, JLAB High School Summer Honors Program Final Report, 2013

Sensitivity	Difference	Correction
$\partial R/\partial x \sim 22$ ppb/nm	< 20 nm	< 440 ppb
$\partial R/\partial \theta \sim 34$ ppb/nrad	< 4 nrad	< 136 ppb
$\partial R/\partial E \sim 0.23$ ppb/ppb	< 100 ppb	< 23 ppb

Table 4: Sensitivities of the scattering rate to beam differences, expected maximum differences, and corrections. The corrections are several orders of magnitude smaller than the asymmetries to be measured.

3.7 Target Density Fluctuations

Density fluctuations in the target add additional noise to the measurement and are therefore undesirable but they don't have any systematic impact. Density fluctuations will be a relatively small effect in this measurement since the statistical width is large. The new GMP-style target design is expected to perform better than previous targets. Fluctuations can be mitigated by increasing flip rate, raster size, or pump speed.

Table 5 shows target density fluctuations as measured in various experiments. The GMP experiment is of most interest because it designed using computational fluid dynamics (CFD) at Jefferson Lab and this is the style of target that would be used in this experiment. GMP was not a parity violation experiment but opportunistic data on the beam and target performance was taken concurrently with the main experiment.

Experiment	I_{beam}	Raster	Reversal	Width
G0	40 uA	2x2 mm	30 Hz	238 ppm
PVDIS	100 uA	4x4 mm	30 Hz	569 ppm
HAPPEX 3	100 uA		30 Hz	1000 ppm
GMP	60 uA	2x2 mm	30 Hz	536 ppm

Table 5: Target density fluctuations as measured in various experiments.

We can attempt to predict what the target fluctuation width will be on a 20 cm GMP-style target in this experiment based on the 15 cm GMP target. The width from density fluctuations scales inversely with raster area. The scaling with beam current is very conservatively assumed to be cubic. We also assume a cubic scaling with target length. Beam energy has a very minor effect on the target and is neglected. Scaling the GMP result to the parameters of this proposal gives,

$$\left(\frac{4\text{mm}^2}{16\text{mm}^2}\right)\left(\frac{70\mu A}{60\mu A}\right)^3\left(\frac{20\text{cm}}{15\text{cm}}\right)^3 536 \text{ ppm} = 504 \text{ ppm}.$$

Table 6 demonstrates the effect of target density fluctuations in this experiment. Assuming density fluctuations at the level of Happex III and a helicity reversal of 30 Hz, the fluctuations increase the statistical uncertainty by 2.6 % of itself. Increasing the reversal rate to 240 Hz decreases the impact to only 0.3 % (assuming a "white" noise spectrum independent of frequency—in practice the target fluctuations decrease with frequency.) The anticipated 504 ppm fluctuation level from the new GMP-style target renders the impact negligible.

Electron rate	Reversal rate	Statistical width	Assumed target width	Relative width increase
800 kHz	30 Hz	4330 ppm	1000 ppm	2.6 %
800 kHz	240 Hz	12250 ppm	1000 ppm	0.3 %
800 kHz	240 Hz	12250 ppm	504 ppm	0.08 %

Table 6: Mitigation of the effect target density fluctuations by increasing reversal rate and using improved target design.

We budget 4 hours to study the target fluctuation properties and choose the helicity reversal frequency for the experiment.

3.8 Backgrounds

3.8.1 Transverse Asymmetry Leakage

Residual transverse asymmetry in the beam can result in an additional parity-conserving asymmetry in the signal. The size of the beam normal single spin asymmetry is not known at these kinematics. This is a dipole asymmetry so the sign and magnitude varies sinusoidally with azimuth. The PVDIS experiment directly measured the transverse asymmetry at those kinematics [32], and found the maximum magnitude to be between 3 and 5 times smaller than the signal depending on kinematics. Compare $A_n \sim 25 \pm 15$ ppm and $A_n \sim 24 \pm 45$ ppm at $Q^2 = 1.1$ and 1.9 GeV^2/c^2 respectively to $A_{PV} \sim -80$ ppm and $A_{PV} \sim -140$ ppm. Taking 8 hours of data with a vertical polarization will allow this to be measured to 7.4 ppm in the SHMS and 14.1 ppm in the HMS.

The vertical spin component will be zeroed to within 2 % using the Mott polarimeter in the source. Propagation through the accelerator and into the hall leaves this component unchanged [33]. Since the SHMS and HMS will not have the same kinematics, the first-order cancellation of this effect is somewhat broken, for vertical polarization. Assuming A_n=25 ppm, with up to 2 % residual transverse polarization, no cancellation in the measurement, and making no correction, leads to a potential uncertainty of 0.5 ppm or 0.4 %.

The horizontal spin component is determined by the spin precession through the accelerator and will be zeroed by doing a "mini spin-dance". Horizontal polarization causes an up-down asymmetry and cancels across the acceptance of each spectrometer, to first order. We assume a factor 10 cancellation of this component. In addition, the acceptance is sensitive to the small magnitude near the zero crossing. The energy of the machine will be monitored throughout the experiment. Changes in energy or energy balance might require changes to the launch or another mini spin-dance.

We budget 0.4 % uncertainty on the transverse asymmetry leakage, 8 hours for direct measurement of A_n with vertical polarization and 8 hours for the mini spin-dance.

3.8.2 Spectrometer Re-scattering

Unlike the HRS dipoles in Hall A there are no magnetized iron "pole tips" in the Hall C spectrometers to scatter off. This removes the danger of large parity-conserving asymmetries arising from spin-spin interactions.

Re-scattering within the spectrometer may cause background with unknown asymmetry in the acceptance. There are no physics processes with asymmetry large compared to the signal that can contribute. This effect will be bounded using a full simulation of the spectrometers and tracking data from early 12 GeV experiments. Specific beam based studies might be necessary during the experiment. We budget 8 hours for such studies.

3.8.3 Target Window Scattering

Scattering from the Aluminum alloy windows causes a small background which needs to be corrected for. The rate was determined using simulation assuming 5 Mil thick entrance and exit windows and the cross section from a global fit [34]. The rate from Aluminum in both spectrometers is <3 % of the total. Figure 8 is the same as Figure 3

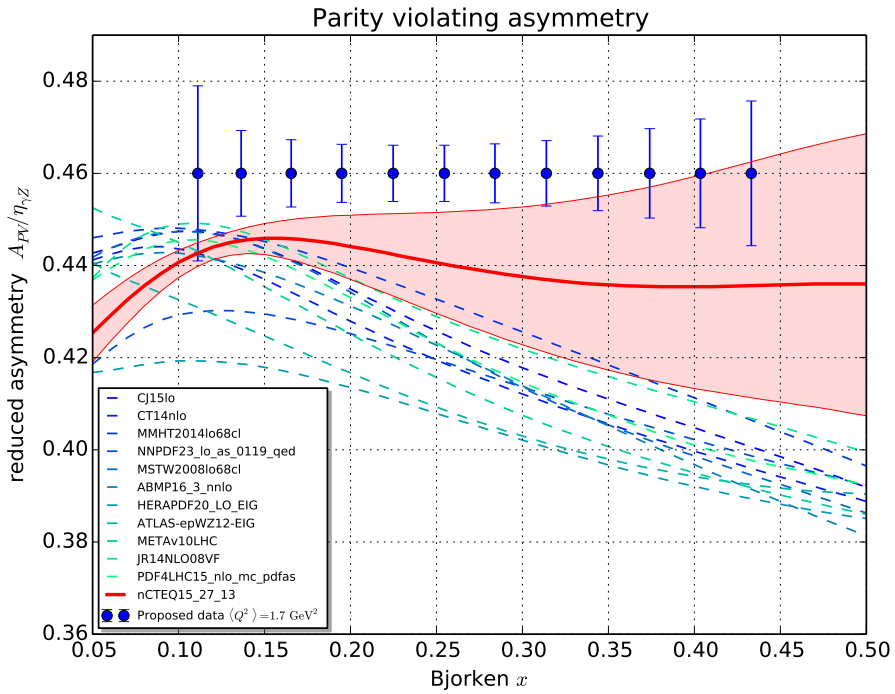

Figure 8: As in Figure 3, with proton asymmetries in blue dashed lines, with the addition of the ^{27}Al asymmetry in red, plotted with uncertainty using the nCTEQ nuclear PDF with Equation (3) for $q \in \{u, d, s\}$.

with the addition of the asymmetry calculated from the nCTEQ nuclear PDF for ^{27}Al. It demonstrates that the asymmetry from Aluminum is expected to be of similar size to that of the proton. Assuming a dummy target with the same thickness (in areal density or fraction of a radiation length) as the hydrogen target and the same beam

current, 24 hours of data will give a precision of ∼5.3 ppm. This beam current will require a special frame for the dummy target to make good thermal contact with the cryogenic target, as was done in the Qweak experiment.

Assuming the target window rate fraction is known to 20 % and the Aluminum asymmetry is different from hydrogen by 20 % and known to 6 ppm this leads to an uncertainty of 0.20 %. We budget 24 hours to measure the asymmetry from a thick dummy target with the same composition as the target windows.

3.8.4 Radiated Elastic Scattering

Elastic scattering that radiates into the acceptance was estimated using the radiative formalism from Mo and Tsai [25]. The rates are found to be ∼4.3 % of the total. The asymmetry was found using the Standard Model and a global fit to the hadronic term [35] and found to be $\sim 60 - 70\%$ of the DIS asymmetry.

Assuming that the rate can be determined to 10 % of itself and the Standard Model asymmetry is known to 5 %, leads to an uncertainty of 0.22 %.

3.8.5 Charged Pion Background

For the purpose of this proposal the cross section for π^- production was determined from the Wiser fit [26] using a radiation length (internal and external) of 0.08.[4] Simulations of pion production show a pion rate only 0.6 of the electron rate at these kinematics. The asymmetry of the pions will be measured concurrently with the electrons—the DAQ and data structure design provides the ability to read out all incident particles. If all the pions are used to measure the pion asymmetry this would have a precision of 1.1 ppm in the SHMS and 2.3 ppm in the HMS. The pion asymmetry is expected to be the same sign and smaller magnitude than the electron asymmetry [32], so that any contamination would serve to decrease the electron asymmetry.

A conservative pion contamination factor of $f_{\pi/e} < 1 \times 10^{-2}$ known to 10 % and a conservatively small asymmetry of 0 ppm, measured to 10 ppm would contribute only 0.08 % to the systematic uncertainty. For reference, the PVDIS experiment obtained pion contamination $f_{\pi/e} < 2 \times 10^{-4}$ with negligible additional uncertainty [32].

3.8.6 Charge Symmetric Electron Background

A charge symmetric background of e^- is produced from the π^0 where a photon converts into e^+e^- pair, and from π^0 Dalitz decay. This background will be subtracted by doing a dedicated direct measurement of the rate and asymmetry reversing the polarity of the spectrometers.

For the purpose of this proposal, the rate of charge symmetric e^- was estimated by assuming that π^0s are produced with a cross section that is the average of the Wiser π^+ and π^- cross sections. The decay electron is assumed to take the full momentum of the mother π^0. A fraction of <0.4 % was determined. This procedure represents an upper bound on the charge symmetric background. The same procedure applied at the kinematics of the E03-103 experiment overestimated this background by a factor 10.[5]

[4] https://github.com/JeffersonLab/remoll/blob/master/include/wiser_pion.h

[5] Private communication, D. Gaskell

The rate of positrons is expected to be so low that a useful measurement of their asymmetry cannot reasonably be performed. The reverse polarity will allow the measurement of the π^+ asymmetry to 11.5 ppm in 8 hours. This combined with knowing the π^- asymmetry can be used to bound the asymmetry in π^0 production.

Assuming an asymmetry half of the signal with 100 % uncertainty, $A_{CS} = 65 \pm 65$ ppm and a fraction of 0.4 % known to 20 % of itself leads to an uncertainty of 0.2 %.

3.9 Systematic Uncertainties

Q^2 determination	0.72 %
Polarization measurement	0.60 %
Residual transverse beam polarization	0.40 %
Dead-time corrections	0.25 %
Elastic radiative tail	0.22 %
Pair-symmetric background	0.20 %
Aluminum endcaps	0.20 %
Beam asymmetries	0.10 %
Pion contamination	0.08 %
Total	1.12 %

Table 7: Table of projected systematic uncertainties. See text for details on the estimation of these quantities.

Table 7 contains a list of the systematic uncertainties and their estimated size. The rationale for each of these estimates is given in the preceding section. The total expected systematic uncertainty of 1.1 % matches very well with the projected statistical uncertainty in the low x region. We emphasize that estimates of the systematic uncertainty are conservative.

3.10 Radiation Estimate

We scale our radiation estimate from an RSAD written for Hall A. For 11 GeV beam of 25 μA on a 1.06 g/cm^2 liquid hydrogen target the prediction is 0.26 μrem/hr dose rate at the fence post. Running for 25 days produced a dose per setup of 157 μrem and 1.6 % of the annual dose budget.

The beam current for this proposal is 2.8 times higher, the target 1.3 times thicker, and the running 1.2 times longer. We include an additional factor of two to account for potential effects from differences between the Hall A and Hall C beam pipes. We estimate 1.9 μrem/hr dose rate at the fence post, a dose per setup of 1372 μrem and 14 % of the annual dose budget.

3.11 Beam-Time Request

We request 38 days to perform an experiment which will significantly constrain the nucleon strange quark PDF. The bulk of the time will be spent on production with

	days	8 hour shifts
Optics and tracking		6
Møller measurements		5
Aluminum target		3
Compton commissioning		3
Pileup monitoring		2.5
Vertical polarization		1
Spectrometer re-scattering		1
Reverse polarity		1
Polarization setup		1
Target fluctuation studies		0.5
Total commissioning and systematics	8	24
Total production	30	
Total	38	

Table 8: Detailed beam-time request.

11 GeV, longitudinally-polarized beam of 70 uA, incident on a 20 cm, liquid-hydrogen target. We devote 8 days to commissioning and to ancillary measurements to constrain systematics. This is composed of time for setup of the beam and polarimeters, tracking mode running to measure the kinematics, measurements of background rates and asymmetries, and a total of just over 2 days for regular measurements of the beam polarization and detector pileup. Table 8 contains the detailed beam-time request with estimates of the various activities.

4 Conclusion

We propose to conduct a parity violation experiment, using the standard equipment in Hall C, which will provide unique, timely, and new information on nucleon Parton Distribution Functions. There are requirements for the beam to have maximum longitudinal polarization in Hall C and some requirements on the "parity quality" of beam. Both polarimeters in Hall C will be needed. The small angles accessible using the magnetic spectrometers allow the measurement to reach down to $x \sim 0.1$ into an important region, not covered by any non-nuclear data, where strange quark distributions are expected to rise rapidly. The DAQ represents the most non-standard item. This will require some R&D work but the performance of previous experiments indicate that this is possible.

In short, this measurement can only be done using the high quality electron beam and experience conducting parity violation experiments available at CEBAF, and the small-angle spectrometers of Hall C. We request a total of 38 days of beam which includes setup and measurement time.

References

[1] J. C. Collins, D. E. Soper, and G. F. Sterman, "Factorization of Hard Processes in QCD," *Adv. Ser. Direct. High Energy Phys.* **5** (1989) 1–91, arXiv:hep-ph/0409313 [hep-ph].

[2] J. Collins, *Foundations of perturbative QCD*. Cambridge University Press, 2013. http://www.cambridge.org/de/knowledge/isbn/item5756723.

[3] C. Alexandrou, K. Cichy, M. Constantinou, K. Hadjiyiannakou, K. Jansen, F. Steffens, and C. Wiese, "New Lattice Results for Parton Distributions," arXiv:1610.03689 [hep-lat].

[4] **New Muon** Collaboration, M. Arneodo *et al.*, "A Reevaluation of the Gottfried sum," *Phys. Rev.* **D50** (1994) R1–R3.

[5] **New Muon** Collaboration, P. Amaudruz *et al.*, "The Gottfried sum from the ratio F2(n) / F2(p)," *Phys. Rev. Lett.* **66** (1991) 2712–2715.

[6] **NuSea** Collaboration, R. S. Towell *et al.*, "Improved measurement of the anti-d / anti-u asymmetry in the nucleon sea," *Phys. Rev.* **D64** (2001) 052002, arXiv:hep-ex/0103030 [hep-ex].

[7] A. W. Thomas, "Chiral Symmetry and the Bag Model: A New Starting Point for Nuclear Physics," *Adv. Nucl. Phys.* **13** (1984) 1–137.

[8] R. Machleidt and I. Slaus, "The Nucleon-nucleon interaction: Topical review," *J. Phys.* **G27** (2001) R69–R108, arXiv:nucl-th/0101056 [nucl-th].

[9] U.-G. Meissner, "Chiral symmetry, nuclear forces and all that," arXiv:1011.1343 [nucl-th].

[10] **European Muon** Collaboration, J. Ashman *et al.*, "An Investigation of the Spin Structure of the Proton in Deep Inelastic Scattering of Polarized Muons on Polarized Protons," *Nucl. Phys.* **B328** (1989) 1.

[11] **NuTeV** Collaboration, M. Goncharov *et al.*, "Precise measurement of dimuon production cross-sections in muon neutrino Fe and muon anti-neutrino Fe deep inelastic scattering at the Tevatron," *Phys. Rev.* **D64** (2001) 112006, arXiv:hep-ex/0102049 [hep-ex].

[12] **NuTeV** Collaboration, M. Tzanov *et al.*, "Precise measurement of neutrino and anti-neutrino differential cross sections," *Phys. Rev.* **D74** (2006) 012008, arXiv:hep-ex/0509010 [hep-ex].

[13] **ATLAS** Collaboration, G. Aad *et al.*, "Measurement of the production of a W boson in association with a charm quark in pp collisions at $\sqrt{s} = 7$ TeV with the ATLAS detector," *JHEP* **05** (2014) 068, arXiv:1402.6263 [hep-ex].

[14] **CMS** Collaboration, S. Chatrchyan *et al.*, "Measurement of associated W + charm production in pp collisions at $\sqrt{s} = 7$ TeV," *JHEP* **02** (2014) 013, arXiv:1310.1138 [hep-ex].

[15] L. T. Brady, A. Accardi, T. J. Hobbs, and W. Melnitchouk, "Next-to leading order analysis of target mass corrections to structure functions and asymmetries," *Phys. Rev.* **D84** (2011) 074008, arXiv:1108.4734 [hep-ph]. [Erratum: Phys. Rev.D85,039902(2012)].

[16] **Particle Data Group** Collaboration, K. A. Olive *et al.*, "Review of Particle Physics," *Chin. Phys.* **C38** (2014) 090001.

[17] A. Buckley, J. Ferrando, S. Lloyd, K. Nordström, B. Page, M. Rüfenacht, M. Schönherr, and G. Watt, "LHAPDF6: parton density access in the LHC precision era," *Eur. Phys. J.* **C75** (2015) 132, arXiv:1412.7420 [hep-ph].

[18] H. Georgi and H. D. Politzer, "Freedom at Moderate Energies: Masses in Color Dynamics," *Phys. Rev.* **D14** (1976) 1829.

[19] R. K. Ellis, W. Furmanski, and R. Petronzio, "Unraveling Higher Twists," *Nucl. Phys.* **B212** (1983) 29.

[20] I. Schienbein *et al.*, "A Review of Target Mass Corrections," *J. Phys.* **G35** (2008) 053101, arXiv:0709.1775 [hep-ph].

[21] T. Hobbs and W. Melnitchouk, "Finite-Q**2 corrections to parity-violating DIS," *Phys. Rev.* **D77** (2008) 114023, arXiv:0801.4791 [hep-ph].

[22] A. Accardi, L. T. Brady, W. Melnitchouk, J. F. Owens, and N. Sato, "Constraints on large-x parton distributions from new weak boson production and deep-inelastic scattering data," *Phys. Rev.* **D93** no. 11, (2016) 114017, arXiv:1602.03154 [hep-ph].

[23] I. C. Cloet, W. Bentz, and A. W. Thomas, "Parity-violating DIS and the flavour dependence of the EMC effect," *Phys. Rev. Lett.* **109** (2012) 182301, arXiv:1202.6401 [nucl-th].

[24] P. E. Bosted and M. E. Christy, "New fits to inclusive electron scattering from proton, neutron, and deuteron at low Q**2," in *Proceedings, 16th International Workshop on Deep Inelastic Scattering and Related Subjects (DIS 2008): London, UK, April 7-11, 2008*, p. 28. 2008. http://www1.jlab.org/Ul/publications/view_pub.cfm?pub_id=8131.

[25] Y.-S. Tsai. Slac-pub-0848, 1971.

[26] D. E. Wiser, *Inclusive Photoproduction of Protons, Kaons, and Pions at SLAC Energies*. PhD thesis, Wisconsin U., Madison, 1977. http://wwwlib.umi.com/dissertations/fullcit?p7719743.

[27] M. Strugari, G. Huber, and W. Li, "Simulations for e/π Separation for the SHMS Heavy Gas Cherenkov Detector," 2016. https://hallcweb.jlab.org/doc-private/ShowDocument?docid=8036.

[28] J. Seely *et al.*, "New measurements of the EMC effect in very light nuclei," *Phys. Rev. Lett.* **103** (2009) 202301, arXiv:0904.4448 [nucl-ex].

[29] A. Narayan *et al.*, "Precision Electron-Beam Polarimetry at 1 GeV Using Diamond Microstrip Detectors," *Phys. Rev.* **X6** no. 1, (2016) 011013, arXiv:1509.06642 [nucl-ex].

[30] K. Paschke, "Controlling helicity-correlated beam asymmetries in a polarized electron source," *Eur.Phys.J.* **A32** (2007) 549–553.

[31] **Qweak** Collaboration, T. Allison *et al.*, "The Q_{weak} experimental apparatus," *Nucl.Instrum.Meth.* **A781** (2015) 105–133, arXiv:1409.7100 [physics.ins-det].

[32] D. Wang *et al.*, "Measurement of Parity-Violating Asymmetry in Electron-Deuteron Inelastic Scattering," *Phys. Rev.* **C91** no. 4, (2015) 045506, arXiv:1411.3200 [nucl-ex].

[33] J. M. Grames, *Measurement of a weak polarization sensitivity to the beam orbit of the CEBAF accelerator*. PhD thesis, Illinois U., Urbana, 2000. http://www1.jlab.org/Ul/publications/view_pub.cfm?pub_id=1126.

[34] P. E. Bosted and V. Mamyan, "Empirical Fit to electron-nucleus scattering," arXiv:1203.2262 [nucl-th].

[35] **Qweak Collaboration** Collaboration, D. Androic *et al.*, "First Determination of the Weak Charge of the Proton," *Phys.Rev.Lett.* **111** (2013) 141803, arXiv:1307.5275 [nucl-ex].